이학 석사 학위논문

Protective effect of extracellular vesicles released from the neural stem cells on 6-hydroxydopamine induced neurotoxicity

6-hydroxydopamine 유도 신경 독성에 대한 신경줄기세포 유래 세포 외 소포체의 신경 보호 효과 연구

2018년 02월

서울대학교 융합과학기술대학원

분자의학 및 바이오제약학과

이 은 지

ABSTRACT

Protective effect of extracellular vesicles released from the neural stem cells on 6-hydroxydopamine induced neurotoxicity

Eun Ji Lee

Department of Molecular Medicine and Biopharmaceutical Science
Graduate School of Convergence Science and Technology
Seoul National University

Neural stem cells (NSCs) are potential therapeutic resources for Parkinson's disease (PD) because they promote recovery of neuronal damage. NSC-secreted extracellular vesicles (EVs) are key mediators of positive paracrine effects. Direct evidence for neuronal protective effects of EVs is

essential for developing new PD therapeutics. In this study, we observed the protective effects of NSC-derived EVs during neurotoxin 6-hydroxydopamine (6-OHDA)-induced degeneration of SH-SY5Y dopaminergic cells. To trace EV movement, a lentivirus containing Palm-tandem dimer tdTomato (Palm-td) was transduced into F3 NSCs. EVs isolated from Palm-td–infected F3 cells showed high tdTomato fluorescence intensity. We found that pre-treatment with EVs dramatically prevented 6-OHDA-induced toxicity by reducing intracellular reactive oxygen species (ROS), percentage of apoptotic cells, and caspase-3/7 activity. These results indicate that NSC-derived EVs have neuroprotective effects against 6-OHDA-induced cell damage, possibly through anti-oxidant and anti-apoptotic action. The findings may provide further insights into potential therapeutic strategies using NSC-derived EVs for neuronal protection against oxidative stress.

Keywords: Extracellular vesicles, Neural stem cell, 6-hydroxydopamine, Protective effect, Parkinson’s disease

Student Number: 2016-26013

TABLE OF CONTENTS

LIST OF FIGURES

INTRODUCTION

Parkinson's disease (PD) is the second most common neurodegenerative disorder, affecting seven to ten million people worldwide. The main pathological feature of PD is a progressive loss of dopaminergic neurons in the substantia nigra pars compacta (SNpc), accompanied by severe deficiency of dopamine concentration in the striatum. Symptomatic motor dysfunction in PD patients appears after about 80% loss of the striatal dopamine terminals [1, 2]. The main clinical symptom of PD is motor impairment, which includes resting tremors, muscular rigidity, and bradykinesia [3]. Increased oxidative stress from mitochondrial dysfunction is also thought to play a role in PD pathogenesis [4].

Although efforts to elucidate the pathogenic progression of PD are ongoing [5, 6], the precise etiology of dopaminergic neurons' degeneration remains unknown. Current treatment options for PD including levodopa, enzyme inhibitors, and deep brain stimulation provide symptomatic relief but do not reverse disease progression [7]. Neuroprotective therapies could

therefore be highly valuable for preventing PD progression. A cure is urgently required to prevent suffering from uninhibited deterioration of motor and non-motor symptoms.

Cell transplantation therapies have been introduced as a promising restorative strategy for PD [8]. Because neural stem cells (NSCs) have the potential to restore lost neuronal cells, they have been considered as influential therapeutic cell sources for neurological diseases [9]. The direct or indirect effects of healthy NSCs that are capable of neurogenesis and of rescuing lost neuronal population may therefore promote the repair of existing damaged tissues. Multiple studies have focused on cell transplantation treatments as a therapeutic option for PD [10-13]. Despite intense research in stem cell therapy, the details of the core biological mechanisms that direct neuronal recovery remain incompletely understood.

Paracrine signaling between implanted stem cells and neighboring host cells offers important clues for functional improvement [14]. NSCs regulate fate specification, differentiation, quiescence, and proliferation through paracrine signaling via transporting vesicles that influence

intercellular condition [15]. Secretome analysis can be used to identify neurotrophic factors that protect injured neurons and promote neuronal growth. It is well known that cells communicate through a variety of methods including soluble factors, surface-associated molecules, and ligand-receptor mediated interactions [16]. In particular, extracellular vesicles (EVs) are known to play a key role in intercellular communication via the transfer of unique molecular signatures that relay the physiological state of producing cells [17-20]. EVs are composed of a lipid bilayer containing diverse types of proteins and RNAs. Stem cell-derived EVs contain a variety of bioactive molecules from their cells of origin that can regulate tissue regeneration [21, 22]. Because the limitations of stem cell transplantation therapy include undesirable tumorigenesis and ethical issues in clinical use, the potential benefits of EVs should be researched concretely to be a robust replacement therapy [23-26]. However, direct evidence of EV-mediated therapeutic effects is lacking.

The oxidative metabolite of dopamine, 6-hydroxydopamine (6-OHDA), is a neurotoxin specific for catecholaminergic cells and is widely

used to produce the pathological condition of PD *in vitro* and *in vivo* [27, 28]. As a hydroxylated analogue of the natural neurotransmitter dopamine, 6-OHDA enters the cells via a dopaminergic re-uptake transporter. SH-SY5Y human neuroblastoma cells are frequently used in PD research because they possess many qualities of substantia nigra neurons [29]. Thus, 6-OHDA treatment of SH-SY5Y cells mimics many aspects of dopaminergic neuronal death in PD. This neurotoxicity of 6-OHDA results in oxidative stresses in the pathogenesis of PD by generating reactive oxygen species (ROS)-related collapses and apoptotic cell death [30, 31].

In light of this evidence, we hypothesized that NSC (HB1.F3)-derived EVs could protect SH-SY5Y cells against 6-OHDA neurotoxicity. The present study investigated whether treating cells with NSC-derived EVs could successfully attenuate the cytotoxic effects of 6-OHDA. We examined EV-related neuroprotective effects by measuring the cell viability, intracellular ROS, the ratio of apoptotic cells, and the level of caspase-3/7 activity.

MATERIALS AND METHODS

Cell culture

Undifferentiated SH-SY5Y cells, a human dopaminergic neuroblastoma cell line and human fibroblast cells were purchased from the American Type Culture Collection (ATCC). HB1.F3 cells, a human fetal telencephalon (15 weeks' gestation) –derived immortal NSC line (kindly provided by Prof. Seung U Kim, Chung-ang university, Seoul, Korea), was cultured in Dulbecco's modified Eagle's Medium (DMEM) supplemented with 10% fetal bovine serum (FBS) and 1% penicillin/streptomycin in a 5% CO_2 atmosphere at 37ºC.

Lentivirus preparation and infection

293FT cells (from ATCC), derived from 293F cells and modified to stably express the SV40 large T-antigen, were plated in a 100 mm^2 dish in DMEM supplemented with 10% FBS. 293FT cells were transfected with

Palm-td lentiviral vector and lentivirus packaging vectors (REV, PMDLg, and Env) using Lipofectamine 2000 and diluted in OPTI-MEM medium (Gibco). Transfected cells were incubated in DMEM supplemented with 10% FBS for 48 hours (h). After supernatant collection, cells and debris were removed by centrifugation at 2000 x g for 30 minutes (min). Purified virus stocks were titrated using the Lenti-X qRT-PCR Titration Kit (Clontech). HB1.F3 cells were plated in a 100 mm^2 dish with 800 μl of fabricated Palm-td lentivirus and 8.8 μl of polybrene (10 mg/ml, Santa Cruz Biotechnology), and were treated with DMEM containing 10% FBS. Completed F3-palm-tdTomato cells were washed with fluorescence-activated cell sorting (FACS) buffer (phosphate-buffered saline [PBS] solution containing 5% fetal bovine serum [FBS]). The collected cells, after centrifugation were resuspended with FACS buffer. The purity of tdTomato fluorescence-positive cells was quantified by FACS (BD Immunocytometry System, CA) analysis.

Assessment of fluorescence intensity stability

F3-palm-tdTomato cells were plated in 24-well plates and 96-well plates and were incubated for different lengths of time (day 1, 3, and 7). Confocal microscopy (Leica Microsystems) and fluorescence microplate reader (Varioskan flash, Thermo scientific) were used to detect fluorescence intensity and stability. F3 cells were used as control.

Preparation and characterization of EVs

EV-depleted FBS was collected by ultracentrifugation at 39800 x g for 16 hours at 4ºC. F3-palm-tdTomato stable cells were incubated in DMEM containing 10% EV-depleted FBS for 48 h. Cells and debris were removed by centrifugation at 2000 x g for 30 min. EVs were isolated using ultracentrifugation at 40000 x g for 3 h and Total EV Isolation kit (Invitrogen) and then resuspended in 1X PBS. The amount of protein was estimated using the bicinchoninic acid assay (BCA; Thermo Scientific). A LM10 nanoparticle tracking analysis (NTA) system (Nanosight) was used to measure EV size

distribution and particle number.

Western blot analysis

Isolated EV concentration was determined using the BCA assay (Thermo Scientific). Equal amounts of protein were resolved by SDS-PAGE and were transferred onto PVDF membranes (Millipore). The membrane was probed with primary antibodies against anti-rabbit CD63 (1:1000 dilution; Santa Cruz Biotechnology) and anti-mouse CD81 (1:1000 dilution; Santa Cruz Biotechnology) overnight at 4ºC. Membranes were incubated with HRP-conjugated anti-rabbit and anti-mouse secondary antibody (1:10000 dilution; Santa Cruz Biotechnology) for 2 h at room temperature (RT, 20 to 23ºC), and proteins were visualized with a chemiluminescence detection system (Promega).

Cell viability assay

SH-SY5Y cells were seeded on 96-well plates and were incubated overnight. After pre-treatment with F3-derived EVs for 30 min, cells were incubated with 6-OHDA (Sigma Aldrich) in 100 μl of media. Cells were incubated for 24 h and cell viability was measured using cell counting kit-8 (CCK-8) assay system (DOJINDO). CCK-8 reagent was added to each well according to the assay protocol and the cells were incubated at 37ºC for 3 h. Absorbance was measured at 450 nm. The values of different absorbance were expressed as a percentage of control.

Measurement of intracellular ROS by fluorescence microplate reader

Cells were pre-treated with F3-derived EVs for 30 min and then incubated with 6-OHDA for 24 h on 96-well plate. Cells were then collected and incubated with 2′,7′-dichlorofluorescein diacetate (DCF-DA, Sigma Aldrich) for 1 h at 37ºC in the dark. The level of intracellular ROS was

quantified in fluorescent microplate reader (485 nm excitation and 535 nm emission, Varioskan flash, Thermo scientific). The measured fluorescence values were expressed as a percentage of the fluorescence in control cells.

Flow cytometric analysis using PI

Cytotoxicity was determined with the propidium iodide (PI) fluorescence method. SH-SY5Y cells were seeded on 6-well plates and were pre-treated with F3-derived EVs for 30 min the next day. Following EV treatment, the cells were incubated with 6-OHDA for 24 h. Then, 1 x 10^6 detached cells were washed three times to remove the medium and were labelled with PI (Sigma Aldrich) for 10 min at RT according to the manufacturer's instruction. After 10 min, cells were analyzed for cytotoxicity with FACS Calibur flow cytometer (BD bioscience). The percentage of PI-positive cells was quantitated with Flow Cytometry Analysis software (Bio-Rad).

Measurement of caspase-3/7 activity

Caspase-3/7 activity was measured with Caspase-Glo 3/7 Assay Systems (Promega) in SH-SY5Y cell line. EV pre-treated cells were incubated with 6-OHDA for 24 h. Next, $1x10^5$ cells were counted and washed with PBS. Caspase-Glo 3/7 reagent was added directly to the cells in 96-well plates and was incubated for 30 min at RT in the dark according to the manufacturer's instruction. Luciferase activity was then measured using Glomax (Promega).

RESULTS

Validation of EV and cell tracing reporter activity in Palm-tdTomato-transduced HB1.F3 stable cell line

To track the behavior of EVs secreted from F3 cells, we labeled multiple EV population with a Palm-td lentiviral vector (Figure 1A). EV budding out from the plasma membrane can then be traced by the tdTomato fluorescence signal. Initially, we transfected HB1.F3 cells with a Palm-td plasmid vector, showing approximately 10% to 20% of the transfected cells. We therefore adopted a lentivirus infection method to enhance intracellular delivery efficacy and long-term transgene expression. We transfected 293FT packaging cells with the Palm-td lentiviral vector to produce virus. We then infected cells with the resultant virus (F3-palm-tdTomato). After F3 cells with fluorescence intensity were sorted, we observed tdTomato fluorescence signals in most F3 cells using confocal microscopy, showing the prominently bright signals in cell membrane area (Figure 1B). FACS (Fluorescence-activated cell sorting) analysis showed that 99% of HB1.F3 target cells (F3

cells) were tdTomato-positive (Figure 1C).

Assessment of the stability of reporter activity in established F3-palm-tdTomato cell line

To verify that established F3-palm-tdTomato cells stably expressed the tdTomato signal, we incubated cells in fluorescence microplate reader and examined them at three successive time points (day 1, 3, and 7). Fluorescence activities were stably maintained in F3-palm-tdTomato cells through 7 days (Figure 2A). Additionally, confocal microscopic images showed that tdTomato was consistently expressed in the F3-palm-tdTomato cells (Figure 2B).

Evaluation of the characteristics of EVs derived from F3 and F3-palm-tdTomato cells

We isolated EVs from F3 and F3-palm-tdTomato cells that had been cultured in DMEM containing 10% EV-depleted FBS. After concentration of

purified EVs were adjusted as 100 μg/ml, we measured the sizes of each isolated EVs with nanoparticle-tracking analysis (NTA). EV sizes were relatively uniformly distributed, with a peak diameter of approximately 120 to 200 nm (Figure 3A).

To determine whether isolated EVs expressed exosomal protein markers including CD63, and CD81, we performed western blot analysis of F3- and F3-palm-tdTomato cell-derived EVs (Figure 3B). Both CD63 and CD81 were expressed in each samples of isolated EVs. The fluorescence signals of isolated EVs were measured using fluorescent microplate reader. EVs isolated from F3-palm-tdTomato cells expressed intense tdTomato fluorescence, compared with that of the background signal of F3 cell-derived EVs. The fluorescence signals were normalized to the background fluorescence intensity of the ultrapure water used to dissolve the EVs (Figure 3C).

SH-SY5Y cells were then treated with the isolated EVs for 24 h. We detected tdTomato expression from EVs inside the SH-SY5Y cells and obtained three-dimensional (3D) images of EV-treated SH-SY5Y cells with

confocal microscopy (Figure 3D).

Pre-treatment with F3-derived EVs prevented 6-OHDA-induced death of dopaminergic cells

The 6-OHDA toxin is frequently used to induce PD-like effects in both *in vitro* and *in vivo* models. We therefore tested the toxic effects of different concentrations of 6-OHDA (100, 200, 300, 400, and 500 μM) on SH-SY5Y human dopaminergic neuroblastoma cells. As expected, 6-OHDA treatment significantly decreased cell viability. The survival rate of SH-SY5Y was approximately 40% when the cells were treated with 500 μM 6-OHDA for 24 h, as compared with that of the vesicle-treated control cells (Figure 4A).

Next, we examined whether EVs secreted from F3 cells can protect SH-SY5Y cells from 6-OHDA-induced damage. EVs were pre-treated for 30 min before 6-OHDA induction. Purified EVs attenuated the 500 μM 6-OHDA-induced cell toxicity in a dose-dependent manner (50, 100, 200, and 400 μg), compared to the group treated only with 6-OHDA (Figure 4B). To preclude

the possibility that F3-derived EVs themselves caused any toxicity to SH-SY5Y cells, the cells were treated with EVs alone and then the cell viability was determined at 24 h later. We did not observe any toxic effects from treatment with EVs alone (at concentrations of 50, 100, 200, and 400 μg; Figure 4C). We also evaluated the effect of human fibroblast cell (HFF)-derived EVs as an additional control. After 30 min of pre-treatment with HFF-derived EVs (at concentrations of 50, 100, 200, and 400 μg), SH-SY5Y cells were incubated with 500 μM 6-OHDA for 24 h. As expected, HFF-EVs did not show a neuroprotective effect against 6-OHDA toxicity (Figure 4D).

Protective effect of F3-derived EVs against 6-OHDA-induced ROS production in SH-SY5Y cells

It has been reported that 6-OHDA-induced neuronal apoptosis is mediated by intracellular reactive oxygen species (ROS) formation due to mitochondrial dysfunction. Because 6-OHDA is a highly reactive substance, which is auto-oxidized and oxidatively deaminated by monoamine oxidase, it

gives rise to ROS. Intracellular ROS level was detected by a DCFH-DA dye, which can be diffused into the cell membrane and deacetylated by esterase to the 2',7'-dechlorodihydrofluorescein (DCFH). As DCFH is converted into the dichlorofluorescein (DCF), it emits fluorescence by ROS. 6-OHDA-induced cells exhibited a significant increase (approximately 2.5 to 4-fold) of DCF fluorescence intensities, compared with untreated cells. The amount of ROS generation increased in a dose-dependent manner (62.5, 125, 250, and 500 μM) following 6-OHDA treatment (Figure 5A). Interestingly, 6-OHDA-induced ROS generation was significantly reduced in cells pre-treated with F3-derived EVs. The production of ROS was gradually decreased by pre-incubation with EVs at the concentration of 50, 100, 200, and 400 μg (Figure 5B).

Neuroprotective effect of F3-derived EVs against 6-OHDA-induced apoptosis of SH-SY5Y cells

We next evaluated whether EV pre-treatment could prevent 6-OHDA-

induced apoptosis of SH-SY5Y cells. We determined the percentage of necrotic cells with a PI staining assay. The population of PI-stained dead cells induced by 6-OHDA increased gradually in a dose-dependent manner (62.5, 125, 250, and 500 μM; Figure 6A). Treatment with 6-OHDA (250 μM) for 24 h increased the percentage of PI-positive cells to 49.2%. In contrast, 6-OHDA-induced apoptosis was attenuated after treatment with F3-derived EVs. The toxin-induced cell death was prevented by F3-derived EV treatment at a concentration of 200 μg, compared with that seen in 6-OHDA–treated cells (Figure 6B, C).

Decreased caspase-3/7 activity in SH-SY5Y cells damaged by 6-OHDA after pre-treatment of F3-derived EVs

While ROS accumulation is known to activate the pro-apoptotic caspase-3/7, 6-OHDA induces over-expression of caspase-3/7 in SH-SY5Y cells. We observed increased caspase-3/7 activity in 6-OHDA dose-dependent manner (50, 100, 200, 400, and 800 μM; Figure 7A). Approximately 1.5-fold

increase was shown at the concentration of 200 μM 6-OHDA, compared with the vehicle-treated cells. However, the caspase-3/7 activity was dose-dependently (50, 100, 200, and 400 μg) suppressed by F3-derived EV (Figure 7B). Interestingly, pre-treatment with F3-derived EVs also reduced caspase-3/7 activity below normal base level of the caspase activity. 2.3-fold inhibition was showed compared with 200 μM 6-OHDA treated cells and 1.2-fold inhibition was showed compared with the vehicle-treated cells. These results reveal that pre-treatment with NSC-derived EVs decreased 6-OHDA-induced activation of caspase-3/7.

FIGURES

A.

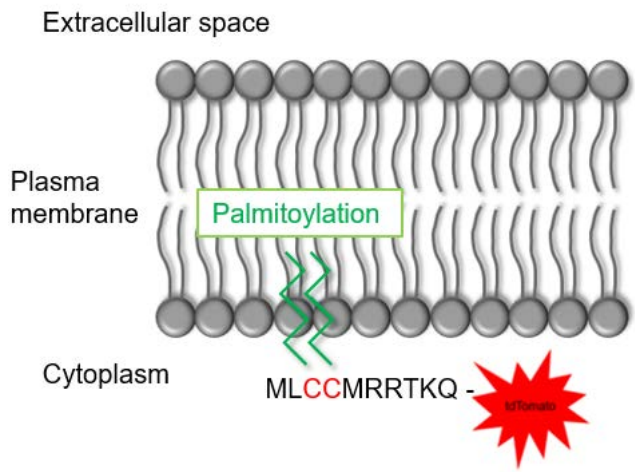
Extracellular space
Plasma membrane
Palmitoylation
Cytoplasm
MLCCMRRTKQ -
tdTomato

B.

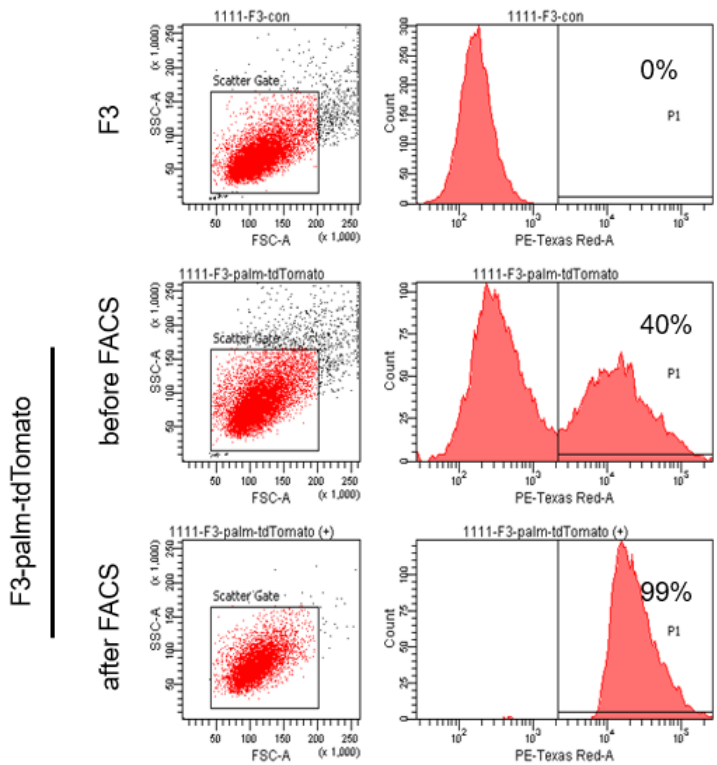
F3-palm-tdTomato
F3
before FACS
after FACS
1111-F3-con
1111-F3-palm-tdTomato
1111-F3-palm-tdTomato (+)
Scatter Gate
SSC-A
FSC-A
(x 1,000)
Count
PE-Texas Red-A
0%
40%
99%
P1

C.

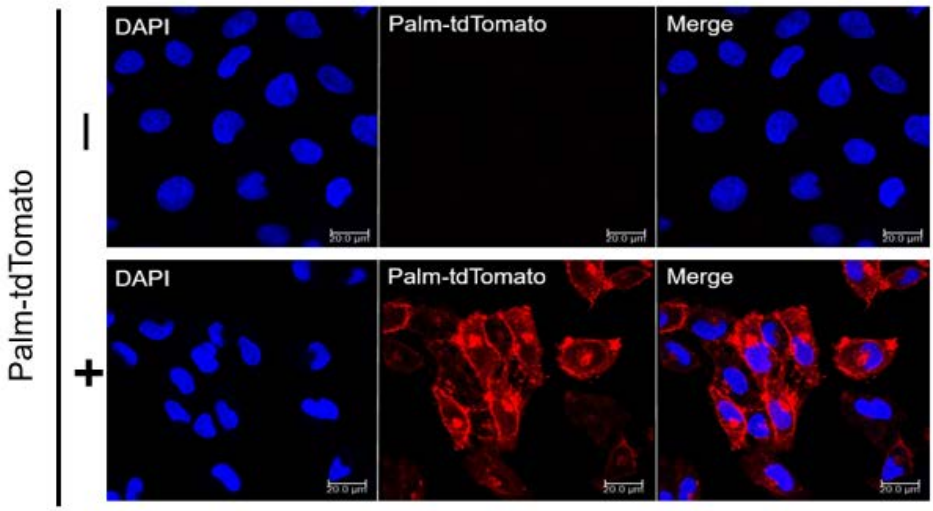

Figure 1. Establishment of F3-palm-tdTomato cell line using a lentiviral system

(A) Schematic diagram of EV membrane labelling with Palm-tdTomato. (B) Palm-td lentivirus was transduced into F3 neural stem cells. 40% of infected F3 cells were Palm-tdTomato positive, and 99% of positively infected F3 cells expressed the Palm-td transgene. (C) Palm-tdTomato-infected F3 cells showed intensively bright signals especially in cell membrane.

A.

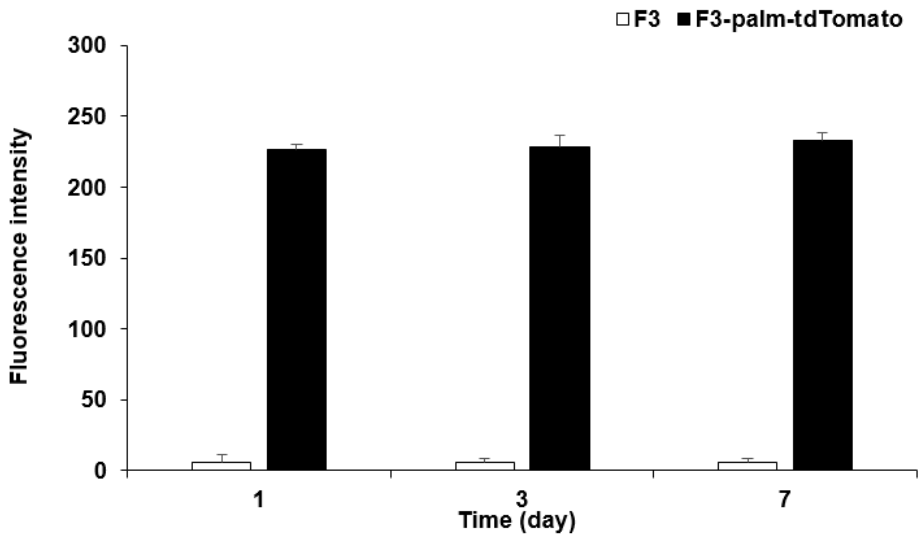
□F3 ■F3-palm-tdTomato
Fluorescence intensity
300
250
200
150
100
50
0
1
3
7
Time (day)

B.

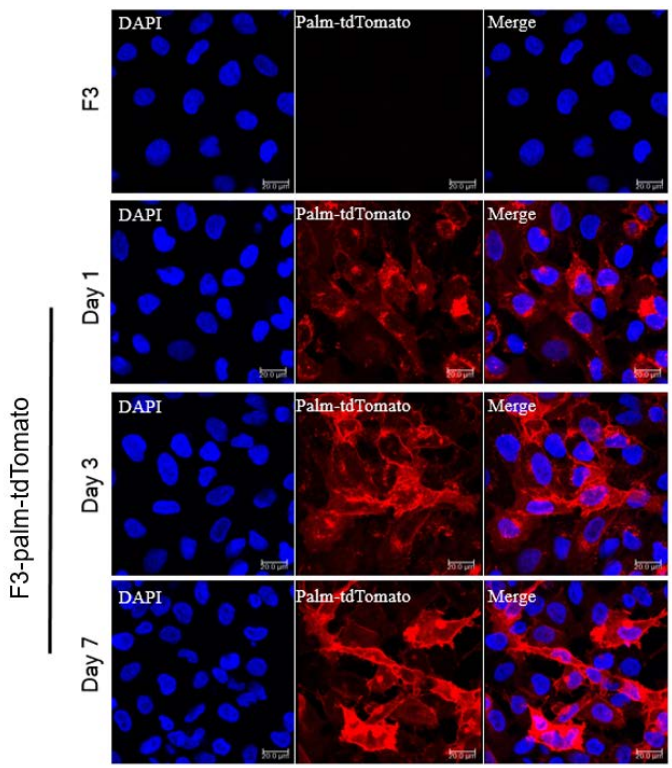
F3-palm-tdTomato
F3
Day 1
Day 3
Day 7
DAPI
Palm-tdTomato
Merge

Figure 2. F3-palm-tdTomato cells maintained stable transgene expression

(A) The tdTomato fluorescence signals in sorted F3-Palm-tdTomato cells were measured using fluorescence microplate reader after 1, 3, and 7 days of incubation. (B) The tdTomato signals of infected F3 cells were still visible at day 7 after incubation. Uninfected F3 cells were used as controls.

A.

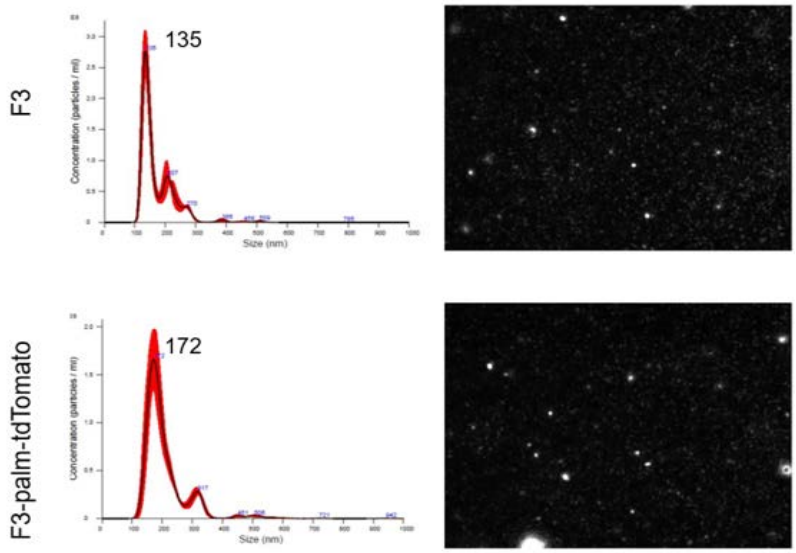
F3
135
Concentration (particles / ml)
Size (nm)
F3-palm-tdTomato
172
Concentration (particles / ml)
Size (nm)

B.

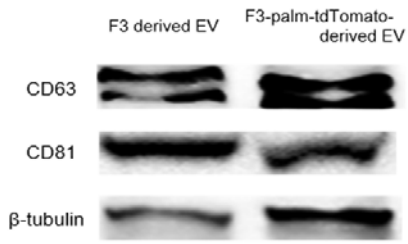
F3 derived EV
F3-palm-tdTomato-derived EV
CD63
CD81
β-tubulin

C.

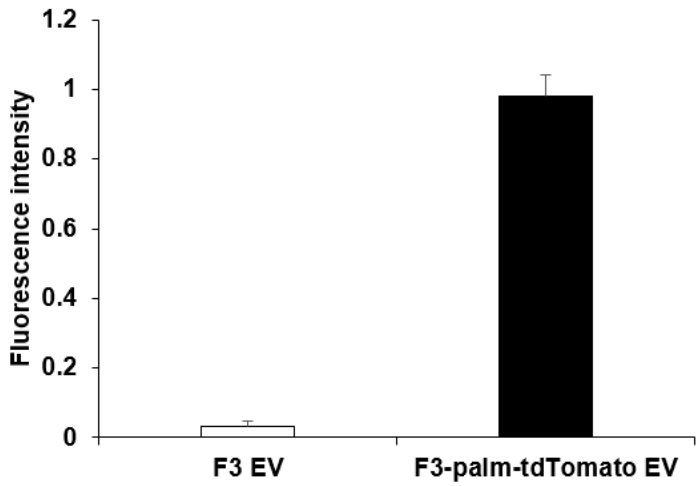
Fluorescence intensity
1.2
1
0.8
0.6
0.4
0.2
0
F3 EV
F3-palm-tdTomato EV

D.

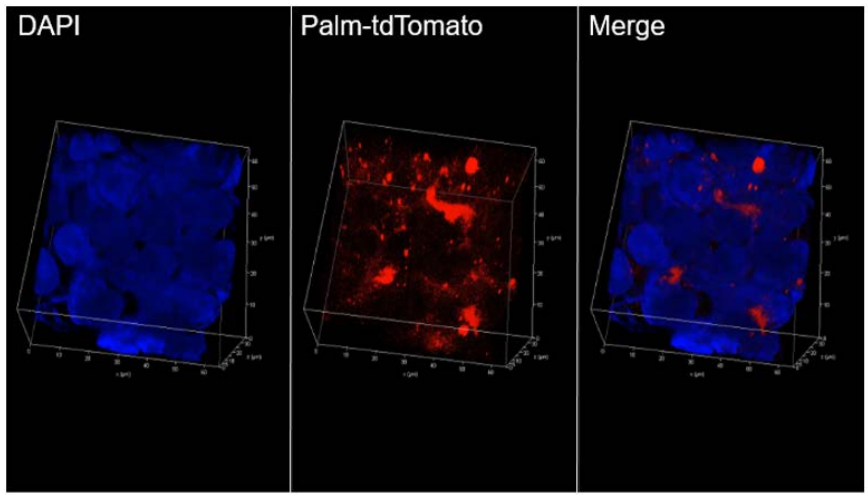

Figure 3. Isolation of F3 palm-tdTomato cell-derived EVs and measurement of their tdTomato signals

(A) To measure EV size, EVs were prepared at a concentration of 100 μg/ml. The size distributions of F3-derived and F3-palm-tdTomato-derived EVs were measured with nanoparticle tracking analysis (NTA). The video clip showed the features of EV particles. (B) Expression of exosomal surface marker proteins CD63 and CD81 was measured using western blot analysis. β-tubulin was used as positive control. (C) F3-palm-tdTomato cell-derived EVs were detected by fluorescence microplate reader, and F3-derived EVs were used as control. Values were normalized to the background fluorescence

signals of ultrapure water. Data are shown in normalized relative fluorescence units. (D) SH-SY5Y cells were treated with isolated F3-palm-tdTomato cell-derived EVs. Fluorescence-traceable EVs were clearly visible via confocal microscopy through live images in video clip.

A.

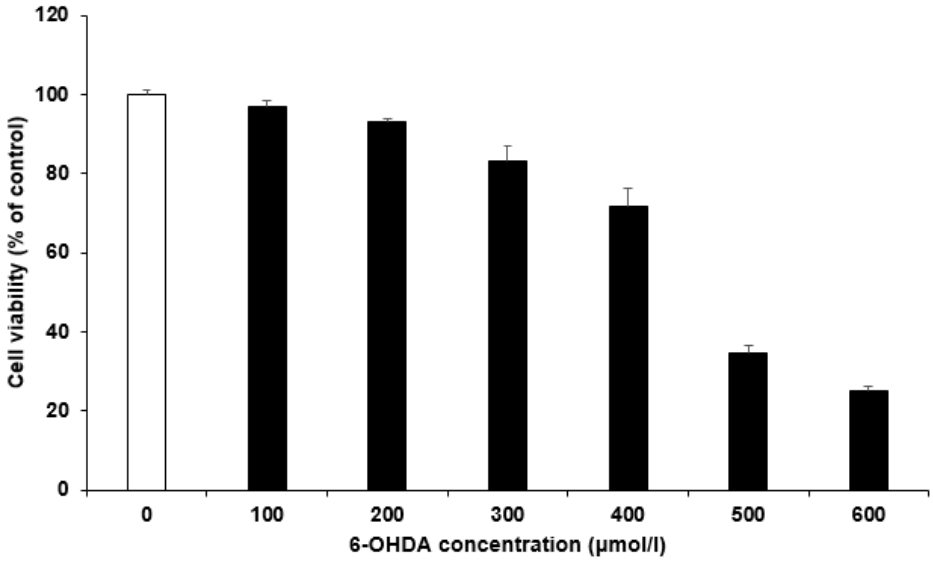
120
100
80
60
40
20
0
Cell viability (% of control)
0
100
200
300
400
500
600
6-OHDA concentration (µmol/l)

B.

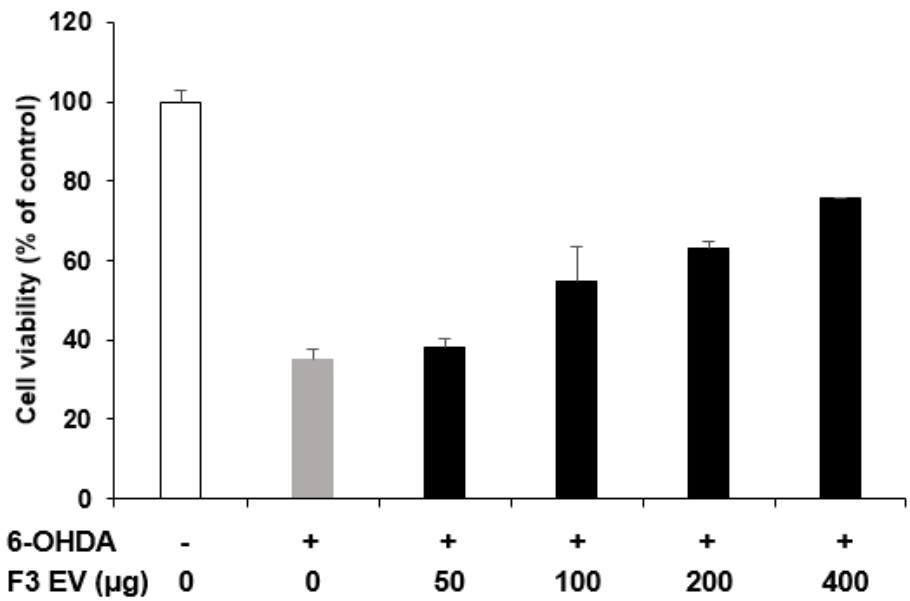
120
100
80
60
40
20
0
Cell viability (% of control)
6-OHDA - + + + + +
F3 EV (µg) 0 0 50 100 200 400

C.

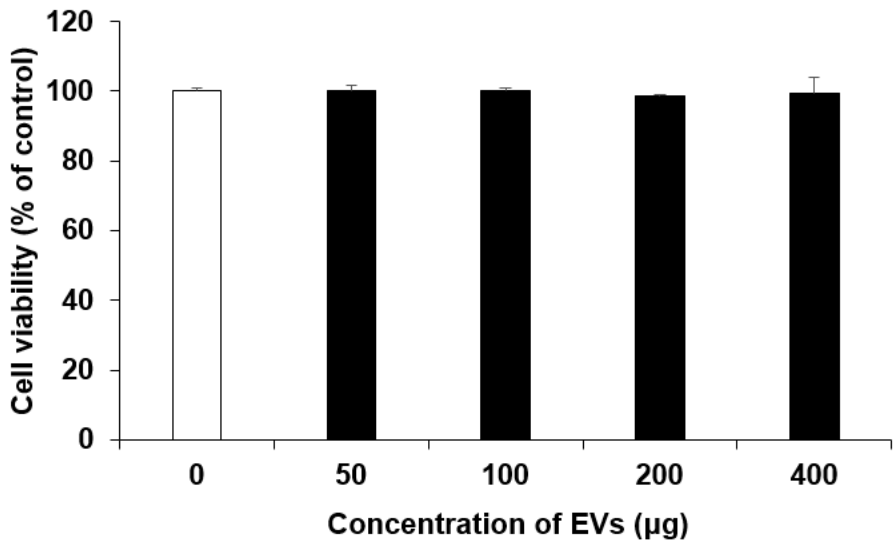
Cell viability (% of control)
120
100
80
60
40
20
0
0
50
100
200
400
Concentration of EVs (µg)

D.

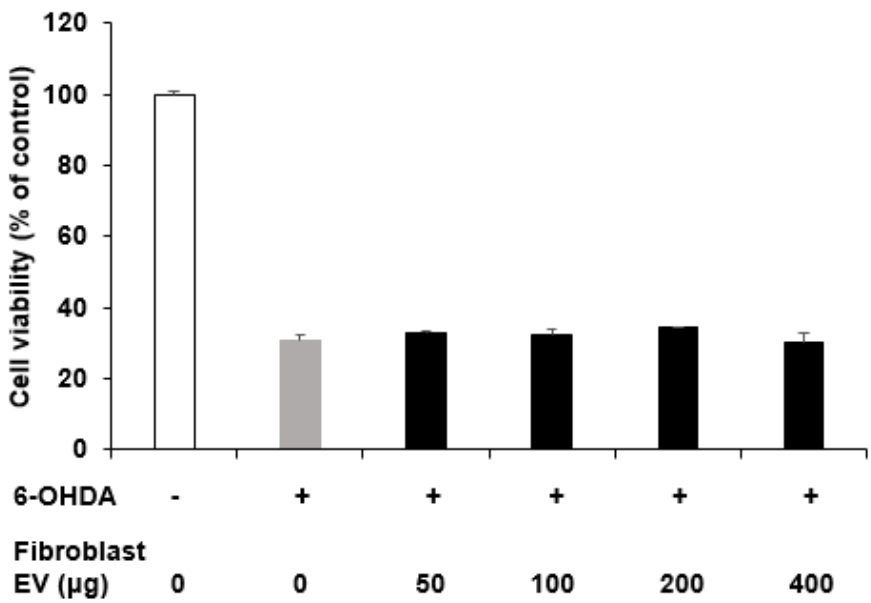
Cell viability (% of control)
120
100
80
60
40
20
0
6-OHDA - + + + + +
Fibroblast EV (µg) 0 0 50 100 200 400

Figure 4. Pre-treatment of F3-derived EVs improved survival of SH-SY5Y cells exposed to 6-OHDA

(A) Cells were treated with various concentrations of 6-OHDA (100, 200, 300, 400, and 500 μM) for 24 h. SH-SY5Y dopaminergic cells showed a concentration-dependent toxicity response to 6-OHDA. (B) Cell survival rates were measured in F3-EV pre-treated cells. Pre-treatment with different concentrations of EVs had protective effect on cells exposed to 500 μM 6-OHDA. (C) The viability of SH-SY5Y cells treated with F3-derived EVs and not exposed to 6-OHDA was measured at the indicated concentrations. (D) As a control, cells were pre-treated with HFF (human fibroblast) cell-derived EVs for 30 min. HFF-secreted EVs did not show a protective effect.

A.

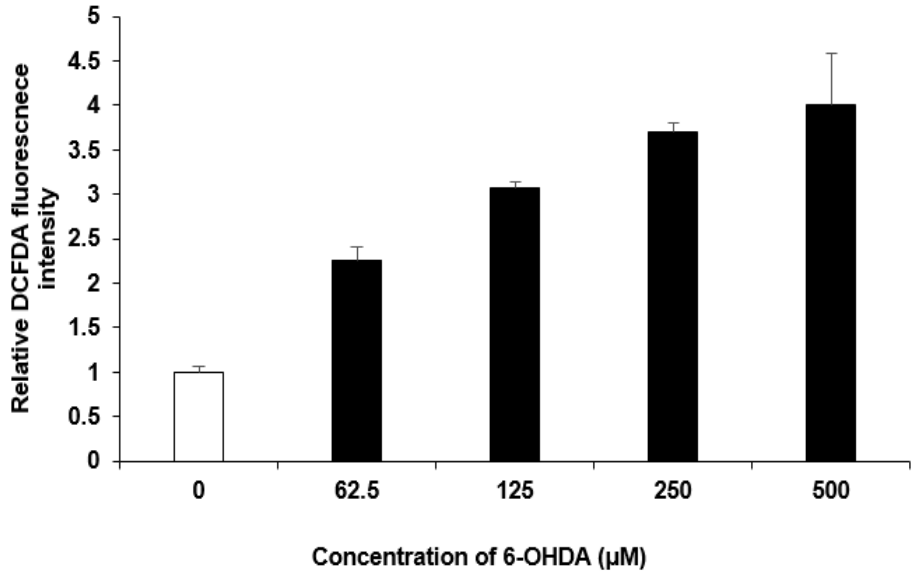
Relative DCFDA fluorescnece intensity
5
4.5
4
3.5
3
2.5
2
1.5
1
0.5
0
0
62.5
125
250
500
Concentration of 6-OHDA (μM)

B.

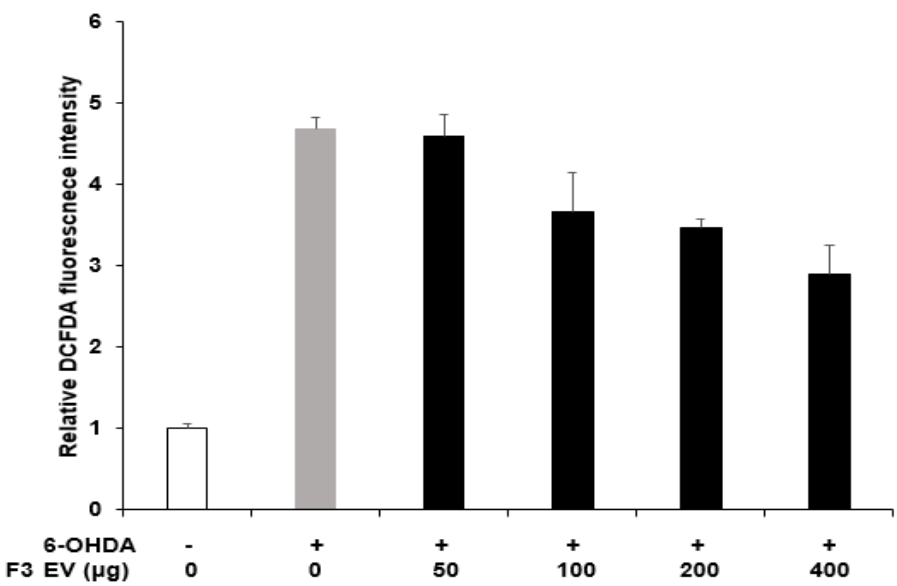
Relative DCFDA fluorescnece intensity
6
5
4
3
2
1
0
6-OHDA - + + + + +
F3 EV (μg) 0 0 50 100 200 400

Figure 5. F3-derived EVs attenuates 6-OHDA-induced intracellular ROS generation

(A) The amount of ROS generated by treating SH-SY5Y cells with 6-OHDA was detected by measuring the fluorescence intensity of DCFH-DA staining. SH-SY5Y cells were treated with different concentrations of 6-OHDA (62.5 μM, 125 μM, 250 μM, and 500 μM) for 24 h. (B) SH-SY5Y cells were pre-treated with increasing concentrations of EVs (50 μg, 100 μg, 200 μg, and 400 μg) for 30 min, followed by 6-OHDA treatment (500 μM) for 24 h. F3-derived EVs against 6-OHDA induced intracellular ROS generation showed a dose-dependent protective effect.

A.

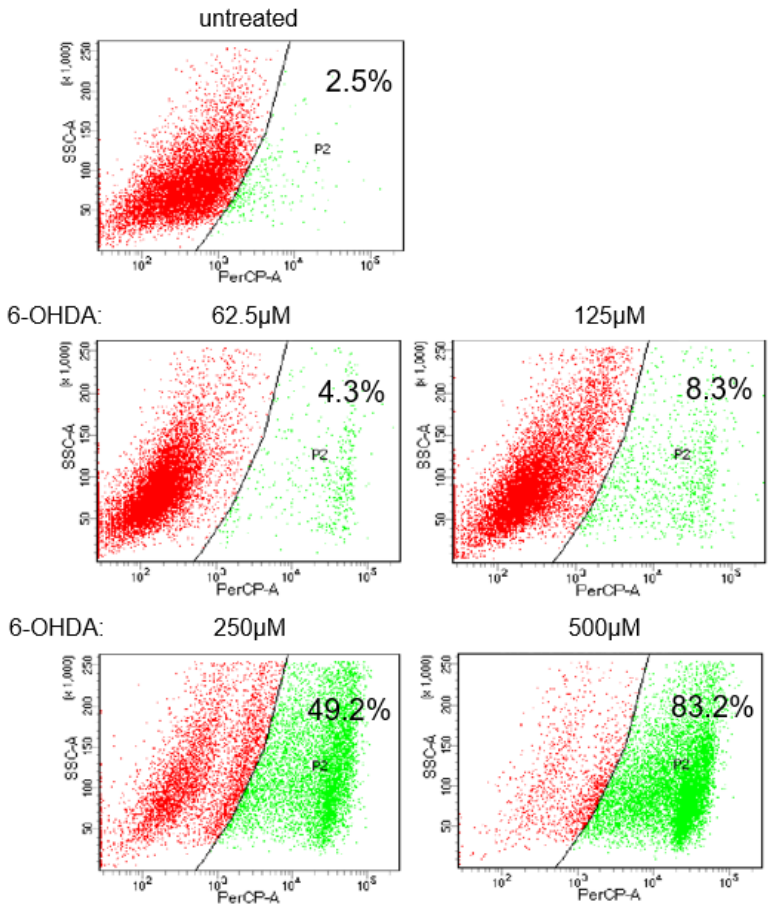

B.

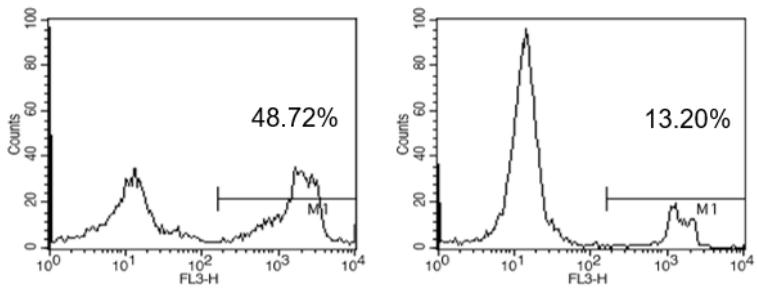

6-OHDA(μM)	**250**	**250**
F3 EV (μg)	**0**	**200**

C.

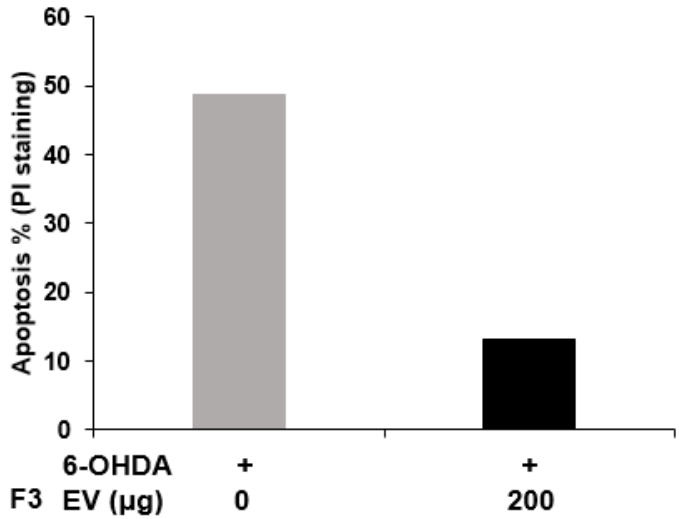

Figure 6. Pre-treatment with F3-derived EVs attenuates 6-OHDA-induced apoptosis of SH-SY5Y cells.

(A) Apoptosis of SH-SY5Y cell was induced by 6-OHDA, illustrated by PI staining and FACS analysis. SH-SY5Y cells were treated with gradually increased concentration of 6-OHDA (62.5 μM, 125 μM, 250 μM, and 500 μM) for 24 h. (B, C) SH-SY5Y cells were pre-treated with F3-derived EVs (200 μg) for 30 min. Then, 6-OHDA (250 μM) was added for 24 h. The apoptotic rate in EV-treated group significantly decreased via PI staining analysis.

A.

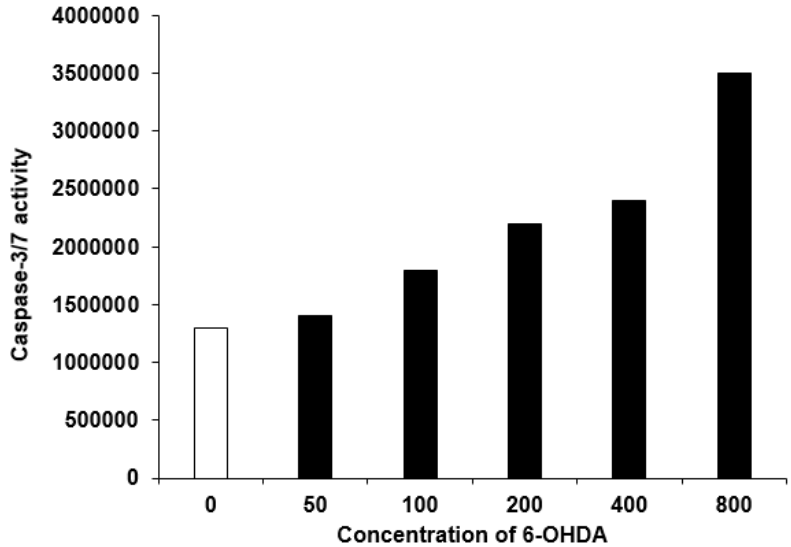
4000000
3500000
3000000
2500000
2000000
1500000
1000000
500000
0
Caspase-3/7 activity
0
50
100
200
400
800
Concentration of 6-OHDA

B.

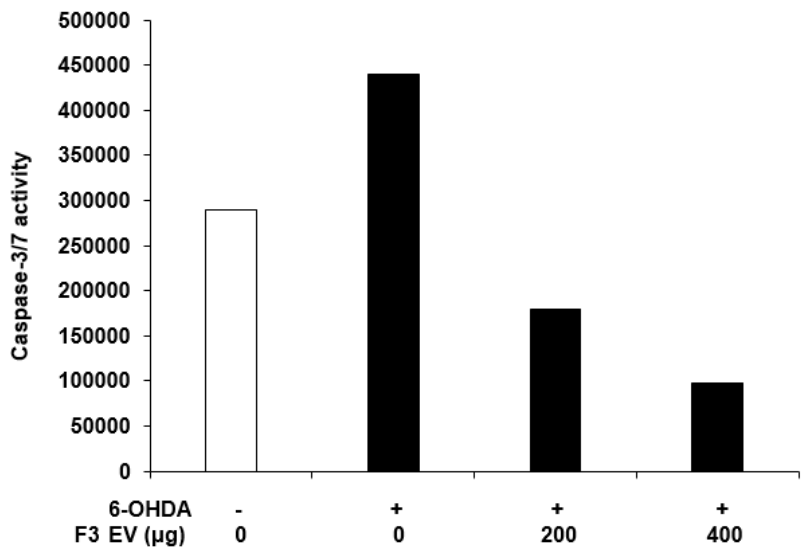
500000
450000
400000
350000
300000
250000
200000
150000
100000
50000
0
Caspase-3/7 activity
6-OHDA - + + +
F3 EV (µg) 0 0 200 400

Figure 7. Treatment with F3-derived EVs decreased caspase-3/7 activity induced by 6-OHDA

(A) 6-OHDA exposure increased caspase-3/7 expression in SH-SY5Y cells after 24 h. Caspase-3/7 activity was measured as a luminescence light unit. (B) Pre-treatment with F3-derived EVs for 30 min reduced caspase-3/7 levels in 6-OHDA-damaged SH-SY5Y cells.

DISCUSSION

Parkinson's disease (PD) is a neurodegenerative disease characterized by bradykinesia, resting tremors, and postural instability. A key symptom of PD is the loss of the nigral dopaminergic neurons and subsequent dopamine deficit in the brain [32]. However, the precise mechanism is still unknown. Dopamine loss in PD is restorable using drugs at present but the effects are only transient. While using stem cells capable of giving rise to dopaminergic neurons is a potential treatment for recovery of damaged neurons [33], such cell replacement therapy still has safety concerns and immunogenic issues. As an alternative therapeutic method, neurotrophic factors secreted by stem cells have been described as increasing the survival rate of neuronal cells and may in fact be a more effective regenerative approach than cell replacement [34, 35].

Neural stem cells (NSCs) may contribute to regeneration from injured brain tissue by their paracrine function. In addition to the release of

diverse factors such as cytokines and chemokines, the cells produce extracellular vesicles (EVs) that transfer RNAs and proteins to recipient cells. NSCs secrete vesicles into the extracellular environment to communicate with neighboring cells [36]. Once released from the donor cell, EVs act as discrete message packets, travelling to proximal and distant recipient cells to alter function and phenotype [37, 38]. The NSC-derived EVs potentially possess stem cell properties capable of accelerating regeneration process, which can be used as alternative therapeutic sources for PD therapy.

Here, we monitored EV trafficking using a Palm-td lentiviral vector in HB1.F3 human NSCs. The thioester linkage between palmitic acid and cysteine enables the fusion of the tdTomato fluorescence protein to the cellular membrane [39, 40]. Fluorescence activity measurement and confocal microscopy showed significantly increased levels of fluorescence after virus infection (Figure 1). We observed small spherical signals around the cell membranes that were predicted to be EVs. EVs produced by the established stable cell line, F3-Palm-tdTomato, maintained their fluorescence intensity for 7 days (Figure 2). Nanometer sizes and exosomal markers were verified

on EVs isolated from F3-Palm-tdTomato cells (Figure 3A, B). We did not observe any significant size differences between EVs from uninfected NSCs and virus-infected NSCs. The fluorescence intensity of F3-palm-tdTomato cell-derived EVs was higher compared with the background signal of the cells (Figure 3C, D). This result indicates that when EVs are secreted from membrane-labeled cells, they bud out of them with the fluorescent tracers inside. From those results, the tracing strategy of EVs endogenously released from cells was established.

A major cause of dopaminergic neuronal loss is oxidative stress that induces neurodegeneration via mitochondrial dysfunction. To produce this pathological condition of PD, 6-hydroxydopamine (6-OHDA) was applied which induces a massive loss of dopaminergic neuron with ROS-mediated oxidative stress [41]. The neurotoxin 6-OHDA is taken up by the cells via dopamine re-uptake transporters and generates intracellular ROS and inhibits mitochondrial function to activate apoptosis cascades. It is commonly used for inducing PD models *in vitro* and *in vivo.* Several studies have demonstrated the usage of 6-OHDA to observe the phenomenon of

degeneration of dopaminergic neurons and to evaluate bioactive compounds as potential treatments for the disease [42, 43].

For our *in vitro* study to examine whether NSC-derived EVs have neuroprotective effects, we treated SH-SY5Y human dopaminergic neuroblastoma cells with 6-OHDA. Concentration-dependent toxicity of 6-OHDA was shown in the result of cell viability examination (Figure 4A). Then, we evaluated the protective effect of NSCs (F3 cells)-derived EVs on 6-OHDA-induced cell damage in SH-SY5Y cells. We observed that pre-treatment of F3-EVs appeared to attenuate 6-OHDA neurotoxicity, while non-NSCs (fibroblast)-derived EVs did not show neuroprotective effects against 6-OHDA neurotoxicity (Figure 4B, D). These data suggest that bioactive components contained in EV derived from NSC, not from fibroblast cells, may play a key role in protecting SH-SY5Y cells against 6-OHDA-induced cell injury. In addition, EV toxicity on the cells was measured and there was no difference on cell viability level, compared with the control cells (Figure 4C). Thus, EV pre-treatment protected dopaminergic cells against 6-OHDA-induced damage without causing any toxicity to the cells. Further study

regarding identification of bioactive molecules contained in NSC-EV needs to be investigated.

Inhibiting reactive oxygen species (ROS) production is an effective strategy to reduce oxidative stress-mediated cell death and to prevent the increase of apoptotic population. While 6-OHDA induces increased ROS production in SH-SY5Y cells (Figure 5A), pre-treatment with F3-derived EVs clearly alleviated 6-OHDA-mediated ROS production. Pre-treatment with EVs for 30 min repressed ROS production in a dose-dependent manner (Figure 5B). From our result showing that the pre-incubation of SH-SY5Y cells with F3 derived EVs effectively prevents 6-OHDA-induced the production of ROS, NSC-EVs that inhibit ROS production might be applied as an important therapeutic agent for neuroprotection.

The generation of intracellular ROS by 6-OHDA is an initial event and finally leads to cell apoptosis. As expected, apoptotic population also increased dose-dependently upon 6-OHDA treatment (Figure 6A). This result indicate that ROS plays an important role in cell apoptosis by neurotoxin 6-

OHDA. Then, we observed that F3-derived EVs attenuated neuronal cell death (Figure 6B, C). To obtain other evidence that EVs protect against neurotoxin-mediated apoptosis, we further investigated the possible signaling mechanisms underlying the protective effect of EVs on 6-OHDA-induced cell injury. Apoptosis is the process of cell death through activation of pro-apoptotic factors such as the caspase cascade. Thus, we focused on the activation level of caspase-3/7 that is a reliable indicator of cell death. 6-OHDA with its different concentrations in SH-SY5Y cells showed the gradually increased activities of caspase-3/7 (Figure 7A). Pre-treatment with EVs and further culture for 24 h showed attenuated caspase-3/7 activation (Figure 7B). These results indicate that EV-mediated neuroprotection likely acts by inhibiting the generation of caspase-3/7, leading to reduce apoptosis induction caused by 6-OHDA neurotoxicity.

In summary, this study demonstrates that NSC-derived EVs protected dopaminergic cells from oxidative insults. Our findings show the potential of EVs as PD therapeutics by showing anti-oxidant and anti-apoptotic effects. While 6-OHDA-induced cell death in SH-SY5Y cells

occurs by the generation of ROS, the neurotoxin-mediated cell death was suppressed by F3-derived EVs via their protective effects on ROS-induced cell damage. We therefore expect that further investigations into the therapeutic applications of NSC-derived EVs will reveal additional advantages for EV-based PD therapies in comparison to cell transplantation.

REFERENCES

1. Wong SL, Gilmour H, Ramage-Morin PL. Parkinson's disease: Prevalence, diagnosis and impact. Health Rep. 2014 Nov; 25(11):10-4.

2. Hornykiewicz, O. Parkinson's disease: from brain homogenate to treatment. Scientific Research. 1973 Fed Proc, 32, 183-190.

3. Magrinelli F, Picelli A, Tocco P, Federico A, Roncari L, Smania N, Zanette G, Tamburin S[1.] Pathophysiology of motor dysfunction in Parkinson's disease as the rationale for drug treatment and rehabilitation. Parkinsons Dis. 2016;2016:9832839

4. Storch A, Kaftan A, Burkhardt K, Schwarz J. 6-Hydroxydopamine toxicity towards human SH-SY5Y dopaminergic neuroblastoma cells: independent of mitochondrial energy metabolism. J Neural Transm (Vienna). 2000; 107(3):281-93.

5. Eriksen JL, Wszolek Z, Petrucelli L. Molecular pathogenesis of Parkinson disease. Arch Neurol. 2005 Mar; 62(3):353-7.

6. Hsiao-Chun C, Christina MU, Robert B. Clinical Progression in Parkinson's Disease and the Neurobiology of Axons. Ann Neurol. 2010; 67:715–725.

7. Katzenschlager R, Lees AJ. Treatment of Parkinson’s disease: levodopa as the first choice. J Neurol. 2002 Sep; 249 Suppl 2:II19-24.

8. Stoker TB, Blair NF, Barker RA. Neural grafting for Parkinson's disease: challenges and prospects. Neural Regen Res. 2017 Mar;12(3):389-392

9. Yasuhara T, Matsukawa N, Hara K, Yu G, Xu L, Maki M, Kim SU, Borlongan CV. Transplantation of human neural stem cells exerts neuroprotection in a rat model of Parkinson’s disease. J Neurosci. 2006 Nov 29; 26(48):12497-511.

10. Napoli E, Borlongan CV. Cell Therapy in Parkinson's Disease: Host Brain Repair Machinery Gets a Boost From Stem Cell Grafts. Stem Cells. 2017 Jun;35(6):1443-1445

11. Hyung-Jun Im, Do Won Hwang, Han Kyu Lee, Jaeho Jang, Song Lee, Hyewon Youn, Yeona Jin, Seung U. Kim, E. Edmund Kim, Yong Sik Kim,

and Dong Soo Lee. *In Vivo* Visualization and Monitoring of Viable Neural Stem Cells Using Noninvasive Bioluminescence Imaging in the 6-Hydroxydopamine-Induced Mouse Model of Parkinson Disease. Mol Imaging. 2013 Jun;12(4):224-34

12. Sundberg M, Isacson O. Advances in stem-cell--generated transplantation therapy for Parkinson's disease. Expert Opin Biol Ther. 2014 Apr; 14(4):437-53.

13. Kim SU, Park IH, Kim TH, Kim KS, Choi HB, Hong SH, Bang JH, Lee MA, Joo IS, Lee CS, Kim YS. Brain transplantation of human neural stem cells transduced with tyrosine hydroxylase and GTP cyclohydrolase 1 provides functional improvement in animal models of Parkinson disease. Neuropathology. 2006 Apr;26(2):129-40.

14. Stefano Di Santo and Hans Rudolf Widmer. Paracrine factors for neurodegenerative disorders: special emphasis on Parkinson's disease. Neural Regen Res. 2016 Apr; 11(4): 570–571.

15. Rhee YH, Yi SH, Kim JY, Chang MY, Jo AY, Kim J, Park CH, Choi JY,

Choi YJ, Sun W, Lee H. Neural stem cells secrete factors facilitating brain regeneration upon constitutive Raf-Erk activation. Sci Rep. 2016 Aug 24;6:32025

16. Felix Scholkmann, Daniel Fels, and Michal Cifra. Non-chemical and non-contact cell-to-cell communication: a short review. Am J Transl Res. 2013; 5(6): 586–593.

17. Raposo G, Stoorvogel W. Extracellular vesicles: Exosomes, microvesicles, and friends. J Cell Biol. 2013 Feb 18;200(4):373-83

18. Tkach M, Théry C. Communication by extracellular vesicles: where we are and where we need to go. Cell. 2016 Mar 10;164(6):1226-1232

19. D. M. Pegtel L. Peferoen, and S. Amor· Extracellular vesicles as modulators of cell-to-cell communication in the healthy and diseased brain. Philos Trans R Soc Lond B Biol Sci. 2014 Sep 26; 369

20. Claudia Bang, Thomas Thum. Exosomes: New players in cell–cell communication. Int J Biochem Cell Biol. 2012 Nov; 44(11):2060-4.

21. Oh HJ, Shin Y, Chung S, Hwang DW, Lee DS. Cell-non-autonomous

neurogenesis by exosome mediated transfer of neurogenic miRNA in microfluidic system. Biomaterials. 2017 Jan;112:82-94.

22. Redmond DE Jr, Bjugstad KB, Teng YD, Ourednik V, Ourednik J, Wakeman DR, Parsons XH, Gonzalez R, Blanchard BC, Kim SU, Gu Z, Lipton SA, Markakis EA, Roth RH, Elsworth JD, Sladek JR Jr, Sidman RL, Snyder EY. Behavioral improvement in a primate Parkinson's model is associated with multiple homeostatic effects of human neural stem cells. Proc Natl Acad Sci U S A. 2007 Jul 17;104(29):12175-80

23. Yongxiang Yang, Yuqin Ye,Xinhong Su Jun He, Wei Bai, and Xiaosheng He. MSCs-Derived Exosomes and Neuroinflammation, Neurogenesis and Therapy of Traumatic Brain Injury. Front Cell Neurosci. 2017; 11: 55.

24. Philipp Pfeifer, Nikos Werner, and Felix Jansen. Role and function of microRNAs in extracellular vesicles in cardiovascular biology. Biomed Res Int. 2015; 2015: 161393.

25. Jialei Yang, Xiufen Zhang, Xiangjie Chen, Lei Wang, and Guodong Yang. Exosome mediated delivery of miR-124 promotes neurogenesis after

ischemia. Mol Ther Nucleic Acids. 2017 Jun 16; 7: 278–287.

26. Liang X, Ding Y, Zhang Y, Tse HF, Lian Q. Paracrine mechanisms of mesenchymal stem cell-based therapy: current status and perspectives. Cell Transplant. 2014;23(9):1045-59.

27. Simola N, Morelli M, Carta AR. The 6-hydroxydopamine model of Parkinson's disease. Neurotox Res. 2007 Apr; 11(3-4):151-67.

28. Mercanti G, Bazzu G, Giusti P. A 6-hydroxydopamine in vivo model of Parkinson's disease. Methods Mol Biol. 2012; 846:355-64.

29. Xie HR, Hu LS, Li GY. SH-SY5Y human neuroblastoma cell line: in vitro cell model of dopaminergic neurons in Parkinson's disease. Chin Med J (Engl). 2010 Apr 20; 123(8):1086-92.

30. Guo S, Bezard E, Zhao B. Protective effect of green tea polyphenols on the SH-SY5Y cells against 6-OHDA induced apoptosis through ROS-NO pathway. Free Radic Biol Med. 2005 Sep 1; 39(5):682-95.

31. Xie L, Tiong CX, Bian JS. Hydrogen sulfide protects SH-SY5Y cells against 6-hydroxydopamine-induced endoplasmic reticulum stress.

Physiol Cell Physiol. 2012 Jul 1; 303(1):C81-91.

32. Shulman JM, De Jager PL, Feany MB. Parkinson's Disease: Genetics and Pathogenesis. Annu Rev Pathol. 2011; 6:193-222.

33. Zhu B, Caldwell M, Song B. Development of stem cell-based therapies for Parkinson's disease. Int J Neurosci. 2016 Nov; 126(11):955-62

34. Anthony DF, Shiels PG. Exploiting paracrine mechanisms of tissue regeneration to repair damaged organs. Transplant Res. 2013;2:10.

35. Pegtel DM, Peferoen L, Amor S. Extracellular vesicles as modulators of cell-to-cell communication in the healthy and diseased brain. Philos Trans R Soc Lond B Biol Sci. 2014 Sep 26;369(1652).

36. Vella LJ, Hill AF, Cheng L. Focus on Extracellular Vesicles: Exosomes and Their Role in Protein Trafficking and Biomarker Potential in Alzheimer's and Parkinson's Disease. Int J Mol Sci. 2016 Feb 6;17(2):173.

37. Zullo J, Matsumoto K, Xavier S, Ratliff B, Goligorsky MS. The cell secretome, a mediator of cell-to-cell communication. Prostaglandins Other Lipid Mediat. 2015 Jul;120:17-20.

38. ArmandoChierchia, NinoChirico, LuciaBoeri, IlariaRaimondi, ,Giovanni A.Riva, ManuelaTeresaRaimondi, MartaTunesi, CarmenGiordano, Gianl uigiForloni, DiegoAlbani. Secretome released from hydrogel-embedded adipose mesenchymal stem cells protects against the Parkinson's disease related toxin 6-hydroxydopamine. j.ejpb.2017.09.014

39. Lai CP, Kim EY, Badr CE, Weissleder R, Mempel TR, Tannous BA, Breakefield XO. Visualization and tracking of tumour extracellular vesicle delivery and RNA translation using multiplexed reporters. Nat Commun. 2015 May 13;6:7029.

40. Kristan E. van der Vos, Erik R. Abels, Xuan Zhang, Charles Lai, Esteban Carrizosa, Derek Oakley, Shilpa Prabhakar, Osama Mardini, Matheus H. W. Crommentuijn, Johan Skog, Anna M. Krichevsky, Anat Stemmer-Rachamimov, Thorsten R. Mempel, Joseph El Khoury, Suzanne E. Hickman, and Xandra O. Breakefield. Directly visualized glioblastoma-derived extracellular vesicles transfer RNA to microglia/macrophages in the brain. Neuro Oncol. 2016 Jan; 18(1): 58–69.

41. Sherri L. Thiele, Ruth Warre, and Joanne E. Nash. Development of a Unilaterally-lesioned 6-OHDA Mouse Model of Parkinson's Disease. J Vis Exp. 2012; (60): 3234.

42. Ning Zhang, Hai-Yang Shu, Tingting Huang, Qi-Lin Zhang, Da Li, Guan-Qun Zhang, Xiao-Yan Peng, Chun-Feng Liu, Wei-Feng Luo, and Li-Fang Hu. Nrf2 Signaling Contributes to the Neuroprotective Effects of Urate against 6-OHDA Toxicity. PLoS One. 2014; 9(6): e100286.

43. Ding YM, Jaumotte JD, Signore AP, Zigmond MJ. Effects of 6-hydroxydopamine on primary cultures of substantia nigra: specific damage to dopamine neurons and the impact of glial cell line-derived neurotrophic factor. J Neurochem. 2004 May;89(3):776-87.